The Solar-B Mission and the Forefront of Solar Physics
ASP Conference Series, Vol. 325, 2004
T. Sakurai and T. Sekii, eds.

Spectroscopic Detection of Magnetic Reconnection Evidence in the Solar Atmosphere with Solar-B/EIS

David H. Brooks, Hiroaki Isobe, and Kazunari Shibata

Kwasan and Hida Observatories, Kyoto University, Yamashina-ku, Kyoto 607-8471, Japan

P. F. Chen

Department of Astronomy, Nanjing University, 22 Hankou Lu, Nanjing, Jiangsu 210093, China

Alessandro C. Lanzafame

Dipartimento di Fisica e Astronomia, Università di Catania, via S. Sofia 78, 95123 Catania, Italy

Abstract. 2.5D MHD simulations of CMEs and flares are combined with improved accuracy density sensitive line emission contribution functions from the ADAS database to study profiles of spectral lines which will fall within the wavelength range of the Solar-B Extreme ultraviolet Imaging Spectrometer (EIS). The objective is to study the signatures of magnetic reconnection associated flow phenomena in the line profiles and provide a set of recommended lines for EIS observations planning. Here, we illustrate our methods by considering the profile of the well-known Fe XII 195 Å line and its ability to detect reconnection inflows. We also discuss the effects of altering simulation parameters such as electron temperature and the inclusion of the effect of heat conduction. The table of recommended lines following these methods is being prepared and will be presented in a separate paper.

1. Introduction

In recent years, a great deal of indirect evidence of magnetic reconnection has been found from EUV and X-ray images of the solar atmosphere. Much of this evidence comes from observations by the Yohkoh satellite, e.g. cusp-shaped expanding post-flare soft X-ray loops (Tsuneta et al. 1992), above the loop-top hard X-ray sources (Masuda et al. 1994), and plasmoid ejections from above the loop-top (Ohyama & Shibata 1998). More recently, Aurass, Vršnak, & Mann (2002) and Aurass (2004 in these proceedings) presented evidence for the detection of the radio signatures of the lower and upper reconnection outflow shocks. In addition, from SOHO-Extreme ultraviolet Imaging Telescope (EIT) observations, Yokoyama et al. (2001) recently found evidence for reconnection inflows. However, to firmly establish the magnetic reconnection model we also require a direct spectroscopic detection of reconnection-related flows since we cannot exclude the possibility of apparent motions in image/movie analysis. For example, as mentioned, Yokoyama et al. (2001) found evidence of reconnection

inflows, but did they detect the inflow itself? Or, an apparent motion due to the rise of the reconnection X-point and associated shock pair? The latter was suggested by Chen et al. (2004) in their reexamination of the same Yokoyama event and a comparison with MHD simulations. If the Chen et al. (2004) interpretation is correct, then the reconnection rate will be underestimated. So, an accurate spectroscopic measurement of the inflow velocities is necessary to remove any ambiguities between real and apparent motions, and to underpin studies of reconnection physics. This is one of the objectives of Solar-B/EIS (Extreme ultraviolet Imaging Spectrometer).

It is of interest, therefore, to investigate which of the spectral lines falling within the EIS wavelength range are most suitable for detecting in/outflows associated with reconnection. Our aim is to provide a table of recommended lines which can be used as an EIS observations planning guide. However, in this short conference report we mainly discuss the methods we employ in our study and present illustrative results for the Fe XII 195 Å line. The complete table of results for a total of 90 spectral lines will be presented in a separate paper (Brooks et al. 2004, in preparation).

2. Atomic Data, MHD Smulations, and Methods

For the atomic data, we used improved accuracy density dependent contribution functions ($G(T_e, N_e)$) from the ADAS database (Summers 2001). These data have been validated in a study of the Differential Emission Measure (DEM) structure of the inner solar corona using 1989 observations by the Solar Extreme ultraviolet Rocket Telescope & Spectrograph (SERTS) (Lanzafame et al. 2002).

For the MHD simulations, the CME and flare models of Chen & Shibata (2000) and Chen et al. (2002) were used. In these models, 2.5D time dependent compressible resistive MHD equations are numerically solved in Cartesian coordinates by a multistep implicit scheme (Hu 1989; Chen, Fang, & Hu 2000). In this work, the initial conditions are almost the same as those of Chen & Shibata (2000). However, here, the effect of gravity is included and the density decreases exponentially with height. Flux emergence near the magnetic neutral line is simulated to trigger the eruption. Magnetic reconnection between the emerging flux and the preexisting coronal field cancels the field lines below the flux rope, leading to the formation of a current sheet as plasma and frozen-in field lines are driven in laterally because of the pressure drop. Fast reconnection thereby sets in, with reconnection inflow driven inward toward the neutral point, and then ejected as reconnection outflow. Above the neutral point, the flux rope system is accelerated and is ejected, while below the neutral point a flaring loop appears, as discussed in detail by Chen & Shibata (2000). Well above the flux rope a piston-driven shock propagates outward.

From this simulation, we obtain the electron density, electron temperature and velocity at each grid point at each time interval. The contribution functions from ADAS were then combined with these results to simulate line profiles integrated along different lines of sight, and to construct intensity images of the simulation domain. Our analysis procedure was as follows:

1) We computed profiles for each line along a chosen line of sight (LOS) inclined at 45 degrees with respect to all three dimensions and passing

through the regions of the reconnection related phenomena in the simulations e.g. the slow mode shock, reconnection inflow, and outflow (for a thorough discussion of these phenomena see Chen & Shibata (2000) and/or Chen et al. (2002)).

2) We computed the intensity distribution in the simulation domain at different wavelengths (velocities).
3) From these results we could easily determine which region contributed the most emission to the intensity at each velocity (see example in the next section).
4) We produced a table classifying each line as suitable (or not) for detecting each flow phenomena.
5) We then examined a subset of these lines comprising the best candidates for detecting a particular flow. We considered criteria such as the line intensity, flow region intensity and whether the flow component would be contaminated by emission from another region along the LOS.
6) For each subset, we computed the line profiles along multiple LOS, to understand the characteristics of the profiles associated with each phenomenon.

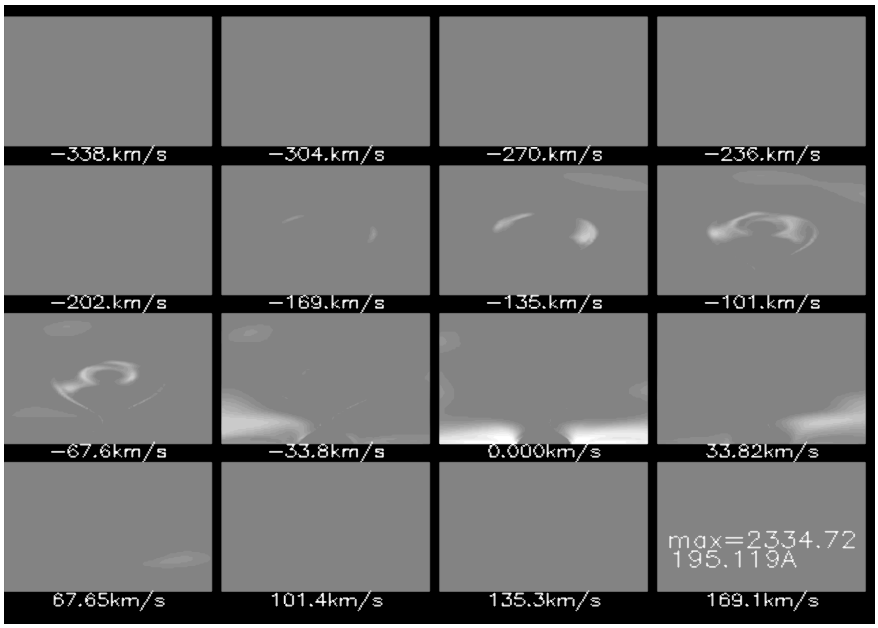

Figure 1. Example of simulated intensity image for Fe XII 195.119 Å. The figure shows the calculated intensity within the simulation domain at different velocities (wavelengths). Here 'max' refers to the maximum intensity of the line.

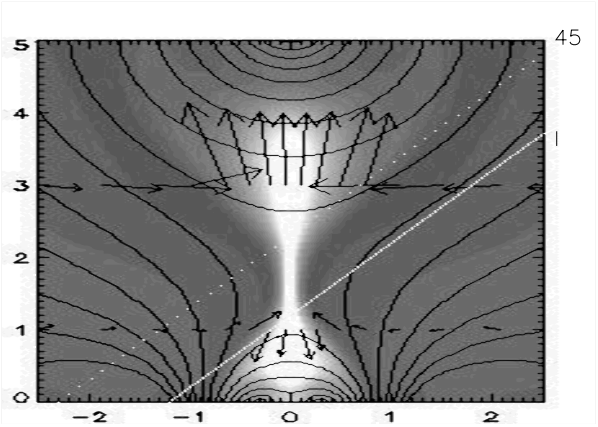

Figure 2. Enlarged cutout of the MHD simulation image showing the chosen line of sight for Figs. 3a and 3b. I – optimized line of sight for reconnection inflow (Fig. 4). 45 – universal 45 degree line of sight.

3. Illustrative Results

To illustrate our methods and results we use the Fe XII 195 Å line as an example. This line is used frequently for observations by SOHO/EIT, TRACE and SOHO/CDS. In Fig. 1 we show the intensity distribution in the simulation domain at different velocities. Here it can be seen that the emission in this line is produced by two distinct components; the reconnection inflow, and the expanding flux rope. The inflow appears to contribute most of the emission in the ± 33 km s^{-1} range and the flux rope contributes most in the 67–135 km s^{-1} range. In principle then, the inflow is distinguishable from the expanding flux rope, so this line was selected as a good candidate under criteria 4) and 5) of the previous section. However, the LOS must be chosen with care.

Figure 2 shows an enlarged snapshot of the MHD simulation domain around the X-point below the expanding flux rope with the original 45 degree LOS (dotted line) and LOS optimized to detect the inflow (solid line) overplotted. The computed line profiles are contrasted in Figs. 3a and 3b, where the normalization unit is 0.9. It can be seen that, along the dotted line, it is difficult to distinguish the blue-shifted inflow emission coming from behind the X-point from the expanding flux rope emission, although we can infer that the highest velocities are associated with the flux rope. However, the inflow in the profile along the optimized LOS (Fig. 3b), with velocities in the range ± 40 km s^{-1}, now appears as a red-shifted hump on the main line profile and contributes 20–30 % to the total intensity. Therefore, in the ideal case where the observations match our theoretical LOS, it is detectable with this line as a *downflow* along the LOS.

4. Parameter Survey

The Fe XII 195 Å line is then, in principle, a good candidate for detecting reconnection inflows with EIS, and through our methods we have identified several

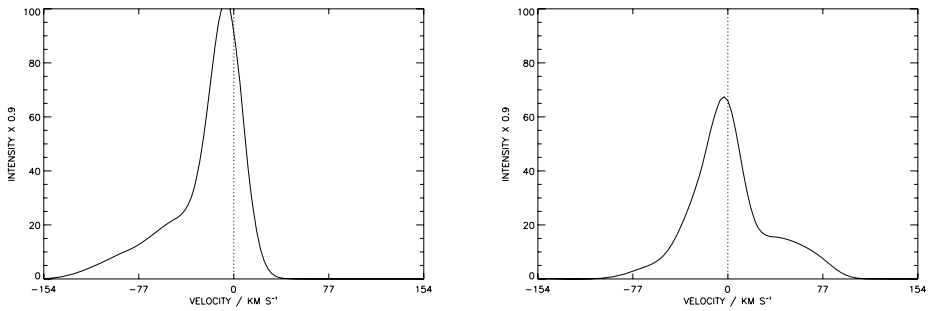

Figure 3. Fe XII 195.119 Å profile showing the signature of the reconnection inflow. a) Left panel: line of sight shown as a dotted line in Fig. 1. b) Right panel: line of sight shown as a solid line in Fig. 1.

candidates for other reconnection related flows. However, an actual detection depends critically on the instrumental characteristics. We are investigating this issue as an extension to this work. In addition, the recommendations of this work obviously depend on the particular simulations performed and so we have further studied the effects of altering various parameters. Figure 4 shows the intensity distribution at 0 km s^{-1} for the same Fe XII 195 Å line (left panel), but also the distribution including heat conduction in the simulations (center panel), and the distribution increasing the temperature by 0.15 in log (right panel).

With heat conduction, the velocity distribution becomes smoother and the inflow appears weaker than before. However, the intensity of the image at this low velocity is now dominated by the post-flare loop which has appeared due to conduction (note the greatly increased max. intensity). By examining the computed line profiles (not shown due to space constraints), we found that the intensity of the central component along the optimized LOS decreases slightly, whereas the inflow component increases slightly and thus contributes a larger fraction of the total intensity. It also becomes more prominent and therefore easier to distinguish. In the higher temperature case (with no heat conduction) the intensity images do not appear much different, but note the increase of the maximum intensity and the apparently stronger emission in the upper left of the image. This is because the simulation temperature is now closer to the formation temperature of the Fe XII 195 Å line ($\log T_e = 6.15$). As a result, both the inflow component and the line intensity itself are a little stronger. These examples demonstrate the sensitivity of the line selection to the model conditions.

5. Summary

By combining 2.5D MHD simulations with improved accuracy contribution functions from the ADAS database we have studied the profiles of spectral lines which will fall within the wavelength range of Solar-B/EIS. The aim was to examine the signatures of magnetic-reconnection-associated flow phenomena and determine the best lines for mass flow detection. 90 spectral lines of different transition types from ions of several elements were considered and the optimal

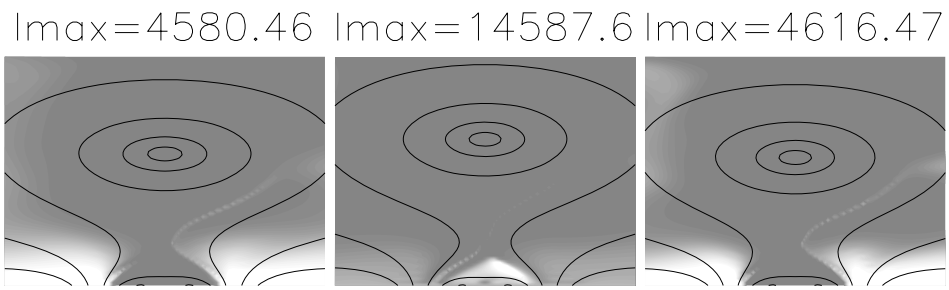

Figure 4. Intensity images in the simulation domain at zero velocity for Fe XII 195 Å. *Left panel*: original simulation. *Center panel*: including heat conduction. *Right panel*: original simulation with T_e 0.15 higher in log. $I_{\max}$ gives the max. intensity in each image.

lines of sight determined. Illustrative results were presented for the Fe XII 195 Å line which was found to be a good candidate for detecting reconnection inflows. However, the likelihood of a real detection depends on the detailed instrumental characteristics of EIS and the particular simulations used. We therefore studied the influence of the simulation parameters on the line selection. In the case of Fe XII 195 Å, we found that including the effect of heat conduction and adopting a simulation temperature close to the formation temperature of the line, helped to distinguish the inflow component from the central line profile. A full report with a definitive set of recommended lines will be given in a forthcoming paper.

References

Aurass, H. 2004, in ASP. Conf. Ser., 000, The Solar-B Mission and the Forefront of Solar Physics: The Fifth Solar-B Science Meeting, ed. T. Sakurai & T. Sekii (San Francisco: ASP), 197

Aurass, H., Vršnak, B., & Mann, G. 2002, A&A, 384, 273

Chen, P. F., Fang, C., & Hu Y. Q. 2000, Chinese Sci. Bull., 45, 798

Chen, P. F., & Shibata, K. 2002, ApJ, 545, 524

Chen, P. F., Shibata, K., Brooks, D. H., & Isobe, H. 2004, ApJ, 602, L61

Chen, P. F., Wu, S. T., Shibata, K., & Fang, C. 2002, ApJ, 572, L99

Hu, Y. Q. 1989, J. Comput. Phys., 84, 441

Lanzafame, A. C., Brooks, D. H., Lang, J., Summers, H. P., Thomas, R. J., & Thompson, A. M. 2002, A&A, 384, 242

Masuda, S., Kosugi, T., Hara, H., Tsuneta, S., & Ogawara, Y. 1994, Nat, 371, 495

Ohyama, M., & Shibata, K. 1998, ApJ, 499, 934

Summers, H. P. 2001, The ADAS Manual v 2.3, `http://adas.phys.strath.ac.uk`

Tsuneta, S., Hara, H., Shimmizu, T., Acton, L. W., Strong, K. T., Hudson, H. S., & Ogawara, Y. 1992, PASJ, 44, L63

Yokoyama, T., Akita, K., Morimoto, T., Inoue, K., & Newmark, J. 2001, ApJ, 546, L69